



Machinability investigation of polymer/GNP nanocomposites in micro-milling

Guoyu Fu¹ · Dehong Huo¹ · Islam Shyha² · Fuzhong Sun³ · Qiang Gao⁴

Received: 19 July 2021 / Accepted: 26 November 2021
© The Author(s) 2021

Abstract

Nanoparticles such as graphene have been added to various polymer matrices to enhance the mechanical, thermal, and electrical properties of polymer materials that require complex designs on a microscopic scale. Micro-machining is used to process these nanocomposite materials to achieve high surface quality and dimensional accuracy while maintaining high productivity. In this study, a systematic micro-milling experiment was performed on polymer/graphene nanoplatelet (GNP) nanocomposites to advance knowledge of the micro-machinability of these materials. It evaluates the effect of the addition of 0.1 wt% GNP nanoparticles on machined surface morphology, chip formation, cutting forces, and tool wear. It is found that the addition of GNP nanoparticles changes the slot edge formation mode from burring mode to chipping mode.

Keywords Machinability · Micro-milling · Polymer · Epoxy/graphene nanoplatelet (GNP) nanocomposites

1 Introduction

A graphene nanoplatelet (GNP) is a flat sheet composed of a single layer of sp^2 bonded carbon atoms, which is considered to be the original structural element of other carbon allotropes, and it exhibits extraordinary mechanical, electrical, and thermal properties [1]. The two-dimensional (2D) structure provides GNP with a much larger specific surface area of $\sim 2600 \text{ m}^2/\text{g}$ compared to other graphene-derived materials [2]. GNP nanoparticles have been experimentally added to various types of polymers such as epoxy, poly(styrene), poly(acrylonitrile) and poly (methyl methacrylate) (PMMA) matrices. Adding GNP to the polymer matrix will cause changes in fracture strain and toughness. In the case of thermoplastic/GNP nanocomposites, the strain at break is

significantly reduced, while for thermoset plastics with low GNP loading, performance is improved [3]. Rafiee et al. [4] showed that GNP exhibits better mechanical reinforcement, including Young's modulus, tensile strength, and toughness, than other graphene-derived nanoparticles. Domun et al. [5] showed that GNP exhibits a higher enhancement of fracture toughness in epoxy-based nanocomposites, mostly at low filler loadings ($< 1 \text{ wt}\%$). Other mechanical tests such as critical buckling load tests and friction tests also show that the addition of GNP nanoparticles can significantly improve mechanical properties [6]. Atif et al. [7] found that the maximum increase in Young's modulus was observed from 609.6 to 766 MPa (25.7% increase) in the case of 0.1 wt% GNP, while Saharudin et al. [8] demonstrated that the addition of GNP nanoparticles (below 1.0 wt%) can increase the glass transition temperature of matrix material, and Aitf et al. [9] found that the addition of GNP can give a maximum increase in hardness up to 18.3% compared with the matrix polymer material. Thus, various improvements in mechanical properties when reinforcing polymers with GNP have been verified.

Based on these properties, polymer/GNP nanocomposites have shown promise for various industrial applications such as in the automobile, mobile phone, and power sectors [10–13]. Although nanocomposite materials can be manufactured close to the final shape, they usually require subsequent machining to achieve the required tolerance and

✉ Dehong Huo
dehong.huo@newcastle.ac.uk

¹ School of Engineering, Newcastle University, Newcastle upon Tyne NE1 7RU, UK

² School of Engineering and the Built Environment, Edinburgh Napier University, Edinburgh EH10 5DT, UK

³ School of Mechanical and Power Engineering, Nanjing Tech University, Nanjing 211816, Jiangsu, China

⁴ School of Mechatronics Engineering, Harbin Institute of Technology, Nan Gang District, 92 West Dazhi Street, PO Box 413, Harbin 150001, China

surface finish [14]. However, research on the machinability of polymer nanocomposites is still ongoing [15]. To accelerate the industrial application of these new materials, the machinability of polymer/GNP nanocomposites needs to be better understood.

The addition of GNP nanoparticles can change the machining performance of the matrix material [16, 17]. Jiao and Cheng [18] demonstrated that the micro-milling strategy for polymer material, which can generate good surface roughness in slot micro-milling, can produce the expected surface roughness on such micro areas, and here, machining dynamics play an important role. Samuel et al. [19] presented a study of the micro-machining of polymer/carbon nanotube nanocomposites which investigated the cutting forces, tool wear, surface roughness, and chip morphology. Xiao and Zhang [16] asserted that the machinability of polymer nanocomposites could be analysed in terms of surface roughness, chip formation, tool wear, gumming and burning. Kobayashi [20] proposed approaches to the study of the cutting performance of polymers, and Patel et al. [21] presented an analysis of the forces on polymer involved in orthogonal cutting or machining in which yielding on a shear plane is assumed. Jiang et al. [22] investigated the relationships among material parameters, such as glass transition temperature, melting temperature, viscous effects and specimen surface finish in polymer machining. Yan et al. [23] conducted micro-milling experiments with various polymers based on surface roughness, burrs and cutting chip characteristics, and it was found that the surface quality of brittle removal is generally better than that of the viscoelasticity state. Aramcharoen et al. [24] demonstrated that the micro-milling method can be used to manufacture microfluidic chips of polymer materials, resulting in good mechanical processing surface quality and a high aspect ratio of about three. Crabtree et al. [25] demonstrated that mechanical processing of polymer materials below the glass transition temperature produces a glassy surface generated by the glassy response. Davies and Burns [26] found that shear bands of polymer materials have a significant impact on the mechanical properties and morphology of the machined surface as well as damaging cutting tools.

Dikshit et al. [27] and Samuel et al. [28] demonstrated that material failure during the machining of nanocomposites is an interface-dominated phenomenon that can change the surface morphology. Kobayashi and Saito [29] showed that GNP nanoparticles can change the friction properties of nanocomposite materials, and these changes directly affect the forming quality of the machined surface. Xu et al. [30] investigated the machinability of CFRP composites using a drilling method, and Le et al. [31] studied the machinability of polymer/carbon nanotube nanocomposites by observing chip formation, surface morphology and cutting force profiles as well as calculating specific cutting energy. For

polymer/GNP nanocomposites, Shakoory et al. [32] presented results showing the effect of tool wear and tool types on machined surface accuracy, while Fu et al. [33] studied the effect of feed per tooth on machined surface accuracy of nanocomposites, and Shyha et al. [34] presented experimental results from the micro-machining of polyester/halloysite nano-clay nanocomposites. The evaluations conducted include the quality of machined surfaces characterised by scanning electron microscopy (SEM), the monitoring of cutting forces using force dynamometry and surface roughness measurement using both contact and non-contact techniques.

The mechanical micro-machining of nanocomposites is a complicated process due to the microstructures of polymer materials. However, research on polymer nanocomposites is still incomplete, particularly in terms of the machinability of polymer/graphene-derived or polymer/GNP nanocomposites. Thus, this study aims to experimentally determine the effect of GNP nanoparticles on the machinability of polymer nanocomposites to fill this gap in knowledge. The micro-machinability of polymer/GNP nanocomposites in this research is characterised by six factors: cutting force, shear stress, surface morphology, chip deformation, slot width accuracy and tool wear.

2 Experimental set-up

2.1 Machining set-up and procedure

The micro-milling experiment was accomplished on an ultra-precision desktop machine (Nanowave MTS5R) with continuous power of 100 W (240 V) and a maximum spindle speed of 80,000 rpm under dry conditions. The device consists of 3 axes (X, Y, Z) with a resolution of 0.1 μm and is controlled by a DC servo motor. A Kistler cutting force dynamometer (9256C2) was used to measure cutting force, as shown in Fig. 1. A light microscope and a scanning electron microscope (Hitachi TM30300) were used to observe the machined surface, slot edge and chip morphology after processing. A Mitutoyo SJ-410 contact style profilometer was used to measure the surface roughness (Ra) of the machined surface. Uncoated flat-end milling tools with a diameter of 1 mm were used in full slot milling. Table 1 lists the specification of the micro end milling tool. To ensure the accuracy of the results, machining trials for each condition were repeated twice.

This micro-milling process can be simplified as an orthogonal machining process, as proposed by Lai et al. [35] for a 2D micro-milling process, as shown in Fig. 1b, c. The maximum uncut chip thickness of 2.0 μm is much smaller than the tool diameter (1000 μm), which results in relatively small variations in uncut chip thickness (2.0 μm) when compared with the travel distance of the cutting edge

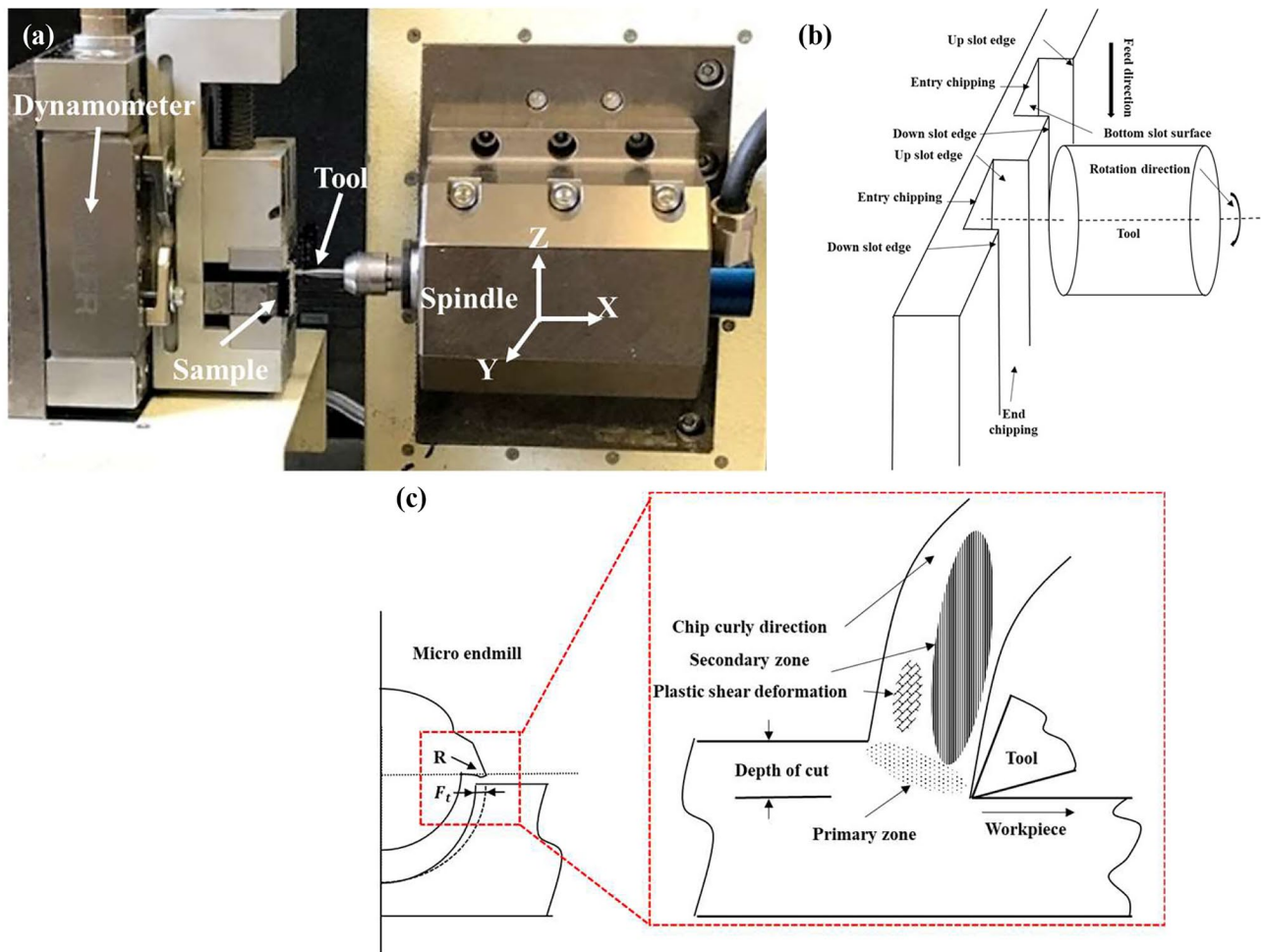


Fig. 1 Micro-milling experiment: (a) machine set-up with cutting force dynamometer; (b) schematic diagram of the 2D milling process of tool rotation; (c) relationship between the 2D milling process and the orthogonal machining process

over 180° of tool rotation (about 1570 μm). Hence, it can be concluded that the change in chip thickness has no significant effect on the impact of cutting force and chip formation. Therefore, the small feed rate in the micro-milling process can be equivalent to the uncut chip thickness used in the orthogonal machining in this study.

The experimental variable in this study is cutting speed. It was set at eight levels (15.7, 31.4, 47.1, 62.8, 78.5, 94.2,

109.9, and 125.6 m/min), and the feed per tooth (FPT) was fixed as 2.0 μm/tooth, as listed in Table 2.

2.2 Workpiece material preparation

The process used in preparing the polymer/GNP material was as follows. Firstly, the GNP nanoparticles were placed in a curing agent by bath sonication at room temperature for 30 min. The suspension and liquid epoxy resin were then mixed with a resin-to-curing agent ratio of 2:1 for 10 min

Table 1 Micro-end milling uncoated tool specifications

Properties	Value
Tool diameter	1.0 mm
Number of flutes	2
Flute style	Right-hand spiral/ medium helix
Finish/coating	Uncoated
Helix angle	30°

Table 2 Experimental cutting parameters

Cutting speed (m/min)	Feed per tooth (μm/tooth)	Tool diameter (mm)	Depth of cut (mm)
15.7, 31.4, 47.1, 62.8, 78.5, 94.2, 109.9, 125.6	2.0	1.0	0.1, 0.2

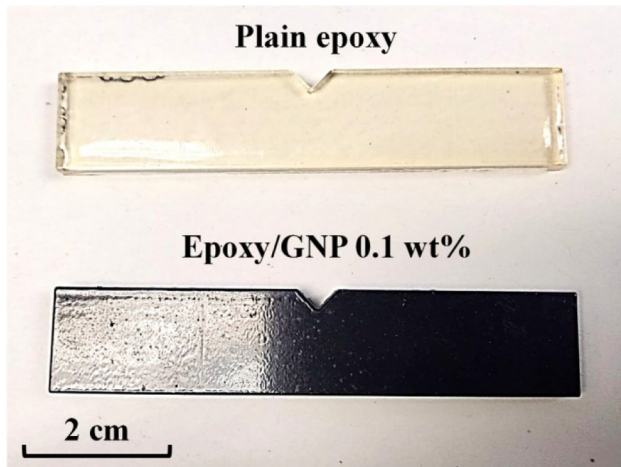


Fig. 2 Epoxy/GNP 0.1wt% nanocomposites and plain epoxy samples for micro-milling experiments

and degassed under vacuum conditions to remove entrained air. Moulding and curing were subsequently conducted at room temperature for 6 h, then curing at 80 °C for 6 h [36]. Figure 2 shows the epoxy/GNP 0.1 wt% nanocomposite and the plain epoxy sample used in this experiment, with the latter as the control.

3 Results and discussion

3.1 Surface roughness (Ra) and surface morphology

Figure 3 shows the surface roughness (Ra) of plain epoxy and epoxy/GNP at cutting speeds from 15.7 to 125.6 m/min at 0.1 mm depth of cut. The experiment results represent the random selection of five points for each experimental condition and taking the average value. Samuel et al. [28] found that the surface roughness of plain polymer decreases with increasing cutting speed. Based on metal nanocomposites, Teng et al. [37] demonstrated the surface roughness of plain Mg and Mg-based metal matrix composites with nano-sized particles. Figure 3 shows that the surface roughness of epoxy/GNP decreases slightly with greater cutting speed. This phenomenon is consistent with the results of previous machining experiments with plain polymer material [38], and the addition of GNP nanoparticles does not change this trend. At the same time, compared with plain epoxy, epoxy/GNP nanocomposites have higher surface roughness. Firstly, the GNP nanoparticles may limit the large long-range mobility of segments of matrix material during the cutting process [39, 40]. As a result, the machined surface of epoxy/GNP has more surface defects, and the surface roughness is higher. The second reason could be that the addition of GNP nanoparticles changes the toughening mechanism of

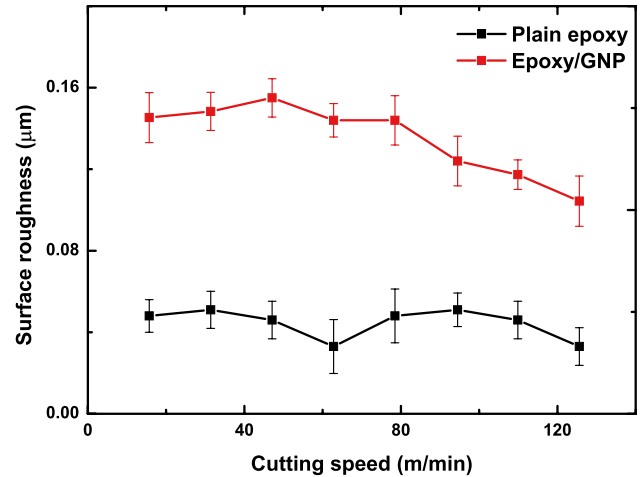


Fig. 3 Surface roughness of plain epoxy and epoxy/GNP at cutting speeds from 15.7 to 125.6 m/min at depth of cut of 0.1 mm

the matrix material [41]. With the addition of GNP nanoparticles, the fracture mode may change from mode I (tension) to mixed-mode (stretch/plane shear and stretch/anti-plane shear) conditions, resulting in higher fracture toughness and increased surface roughness [41, 42].

Figure 4a shows SEM images of the machined surfaces of plain epoxy and epoxy/GNP at cutting speeds of 15.7, 78.5, and 125.6 m/min. The epoxy/GNP surface presents many tears and scaling and a rough pitted appearance. Plain epoxy and epoxy/GNP show different surface morphological characteristics, because the plain epoxy shows signs of brittle fracture and the effect of crack propagation caused by stress concentration [34, 43]. As shown in Fig. 5, a river-like fracture pattern can be observed on the epoxy surface, which illustrates the brittle fracture nature of the material and its poor resistance to crack initiation and propagation [36]. For various epoxy/GNP materials, the fracture pattern changes to a sheet-sheet delaminating pattern [36].

It is believed that this change can produce significantly increased fracture toughness. The addition of 0.1wt% GNP particles does significantly increase the fracture toughness of the matrix material [39], as shown in Fig. 6. As a result, the fracture mode of the machined surface changes from mode I to mixed mode [7], eventually leading to changes in the surface morphology of the machined surface. Figure 4b shows optical images of the machined surfaces of plain epoxy and epoxy/GNP at cutting speeds of 15.7, 78.5, and 125.6 m/min. This further indicates that the addition of GNP nanoparticles changes the surface morphology.

Figure 7 shows SEM images of the different slot edge formation of plain epoxy and epoxy/GNP at cutting speeds of 15.7, 78.5, and 125.6 m/min. Edge chipping defects are observed in epoxy/GNP slots and edge burrs in the plain epoxy samples. This may be because the GNP

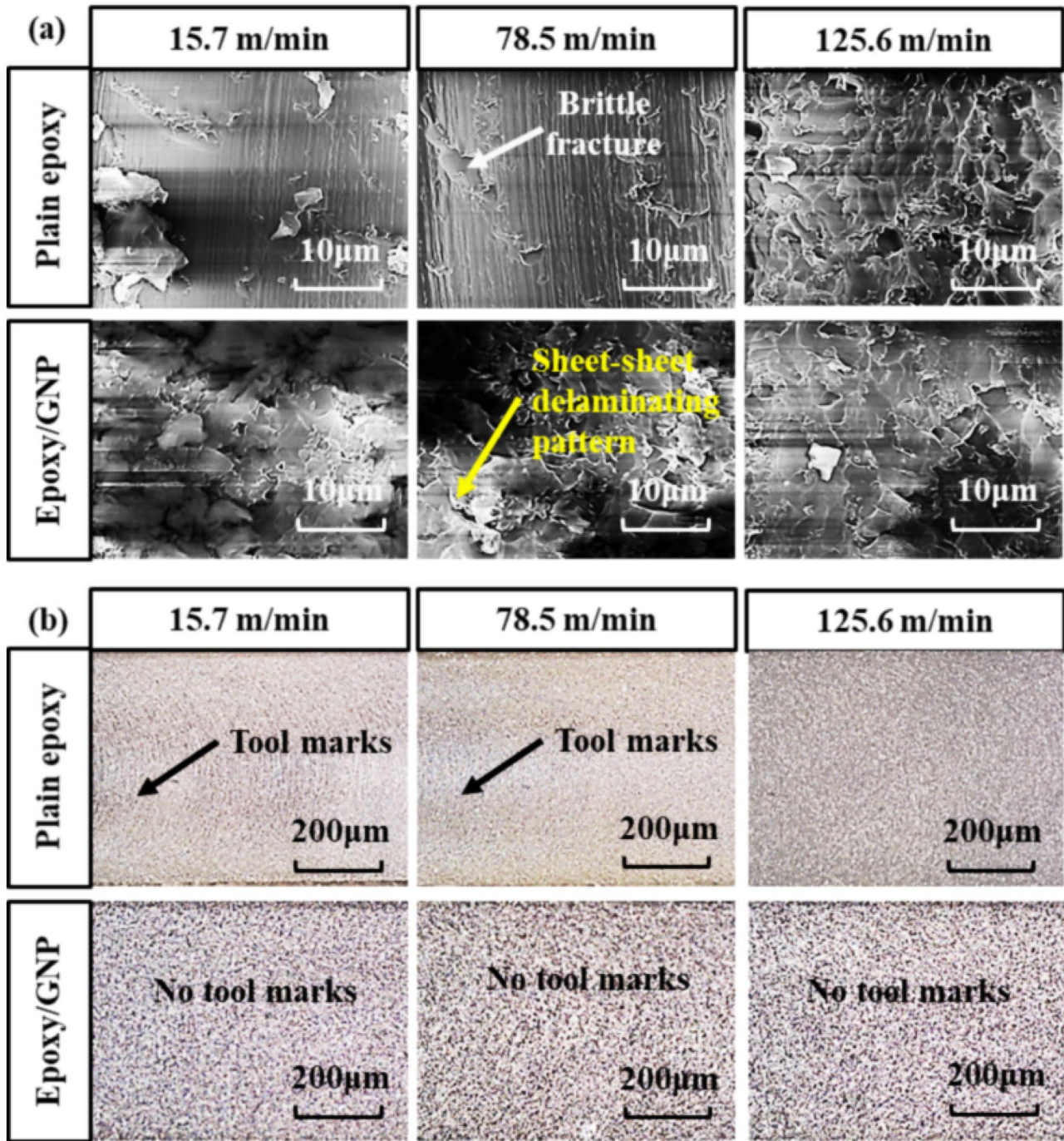
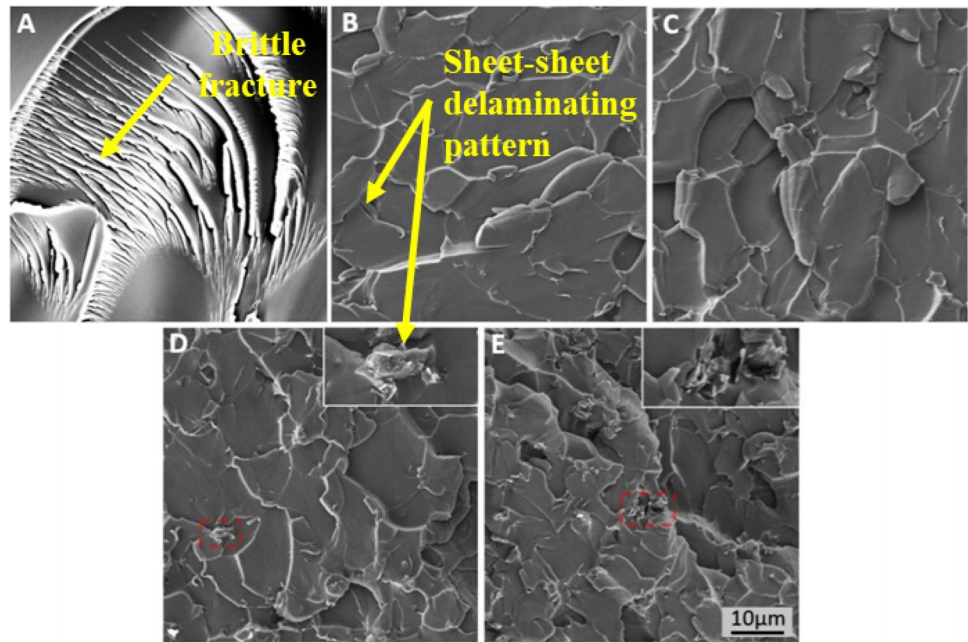


Fig. 4 Machined surfaces of plain epoxy and epoxy/GNP at cutting speeds of 15.7, 78.5, and 125.6 m/min and 125.6 m/min at 0.1 mm undeformed chip thickness: (a) SEM images; (b) optical images

nanoparticles provide a physical barrier to fractures during the cutting process [7]. Their addition means that the slot edge suffers highly concentrated stress and crack growth, and the slot edge formation changes from burred to chipping edges. The change in the mode of breakage of the slot edge is observed at all different cutting speeds tested.

Slot width can directly reflect a component's dimensional accuracy. Therefore, this study investigated the effect of GNP nanoparticle content on slot width. To ensure the accuracy of the results, five points are randomly selected in each slot, the width of the slot is measured, and the average value is calculated. Figure 8

Fig. 5 SEM images of fracture surfaces: (a) plain epoxy; (b) epoxy/GNP 0.1wt%; (c) epoxy/GNP 0.3wt%; (d) epoxy/GNP 0.5wt%; and (e) epoxy/GNP 1.0wt%. Reproduced from [36]



presents optical images of micro-machined slots for plain epoxy and epoxy/GNP nanocomposites at different cutting speeds, and Fig. 9 shows the variations in slot width for both materials at the same cutting speeds at a cutting depth of 0.1 mm. The addition of GNP nanoparticles leads to only a slight decrease in slot width. This small difference will not significantly improve machining accuracy and may occur because the addition of GNP nanoparticles reduces the friction coefficient during processing so that less frictional heat is generated, thereby leading to small changes in shape during machining.

Another reason is that the 0.1 wt% GNP nanoparticles in the epoxy matrix can improve the thermal conductivity [36] of the matrix material during the entire cutting process,

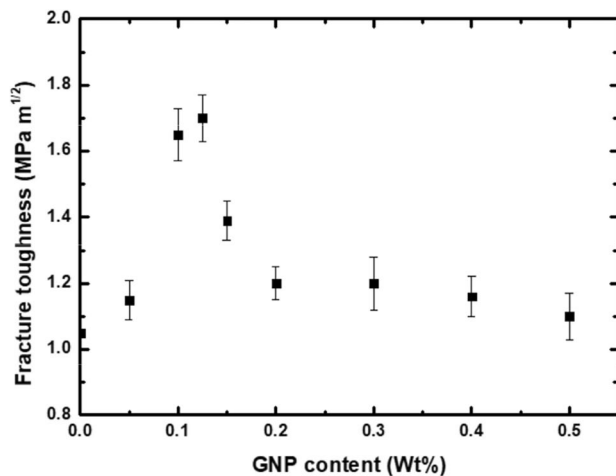


Fig. 6 Fracture toughness plotted as a function of GNP (wt%) in the epoxy matrix, adapted from [39]

thereby increasing the dimensional accuracy of the features produced. Schaller et al. [44] concluded that the increase in thermal conductivity can provide better dimensional accuracy.

3.2 Chip formation

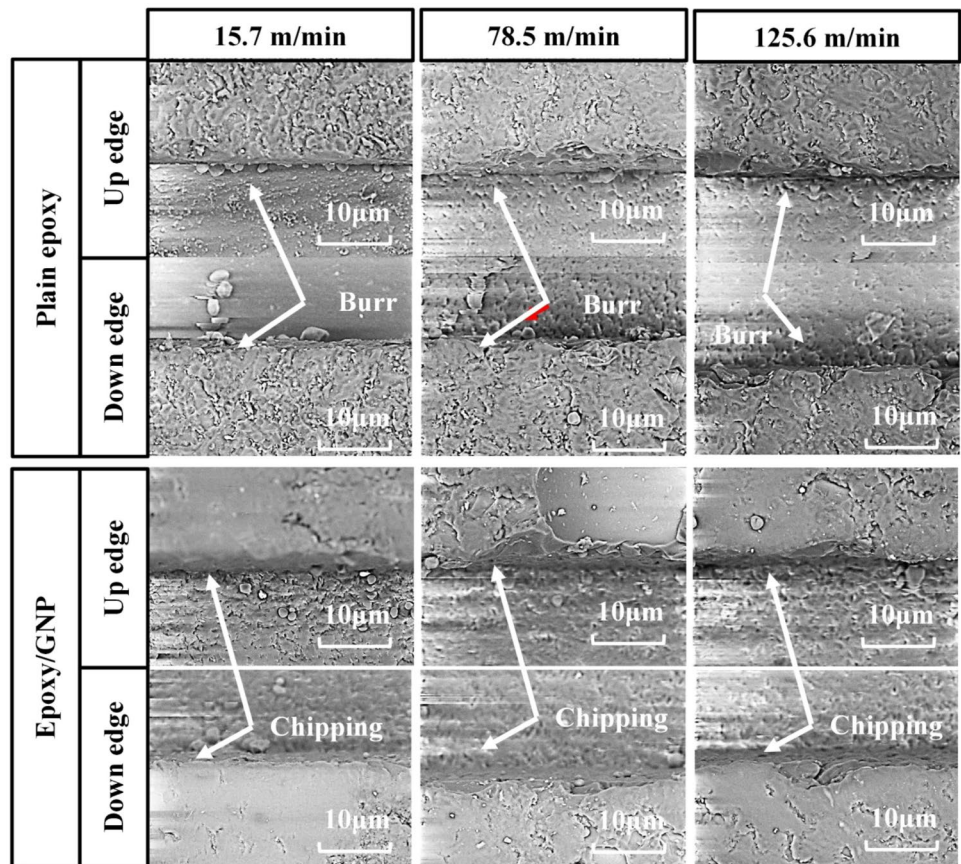
Figure 10a shows SEM images of plain epoxy and epoxy/GNP chips collected after cutting at speeds of 15.7, 78.5, and 125.6 m/min, while Fig. 10b shows SEM images of the surface of the chips. Both materials exhibit continuous chips at all cutting speeds, with no noticeable differences between them. As the cutting speed increases, the chip lengths for both materials increase. This may be due to the phenomenon of the cross-linking of bonds in the thermosetting epoxy which softens with increasing cutting speed [29, 45], thus helping to form complete chips during the cutting process.

However, this study did not find a rubbery plateau region in the cutting process, which has been reported to occur when the cutting temperature exceeds the glass transition temperature T_g , and the epoxy becomes a rubber-like material characterised by high elongation and elasticity at break and a low modulus, with tiny chips almost like dust [46]. Below T_g , good surface quality can be obtained.

3.3 Cutting force

Resultant average cutting force is the primary metric in the analysis of material machinability. The cutting tool's relative motion directly generates a cutting force on the work-piece during machining. It occurs in the same direction as the movement of the cutting tool. Using the computed thrust

Fig. 7 SEM images of slot edges of plain epoxy and epoxy/GNP at cutting speeds of 15.7, 78.5, and 125.6 m/min at 0.1mm depth of cut



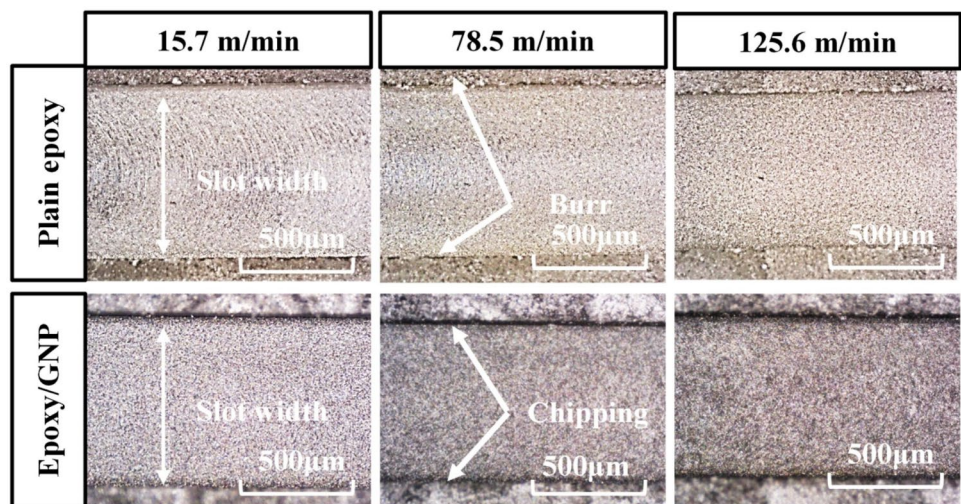
force, F_t , and the cutting force, F_c , the resultant cutting force F_r can be calculated using Eq. 1 [47]:

$$F_r = \sqrt{F_t^2 + F_c^2} \quad (1)$$

Figure 11 shows the effect of cutting speeds on the cutting force of plain epoxy and epoxy/GNP at depths of cut of 0.1 mm and 0.2 mm. For both plain epoxy and epoxy/GNP

nanocomposites, the cutting force is observed to fall from 15.7 to 47.1 m/min as cutting speed increases. A further increase in cutting speed appears to boost and then reduce the cutting force for both materials. This ‘fall-rise-fall’ trend of cutting force against cutting speed is similar to the behaviour of thermosetting polymer in macro milling [48, 49]. Increased cutting speed raises the strain rate of deformation, where the strain hardening and thermal softening of

Fig. 8 Optical images of whole slots in plain epoxy and epoxy/GNP nanocomposites at cutting speeds of 15.7, 78.5, and 125.6 m/min at 0.1 mm undeformed chip thickness



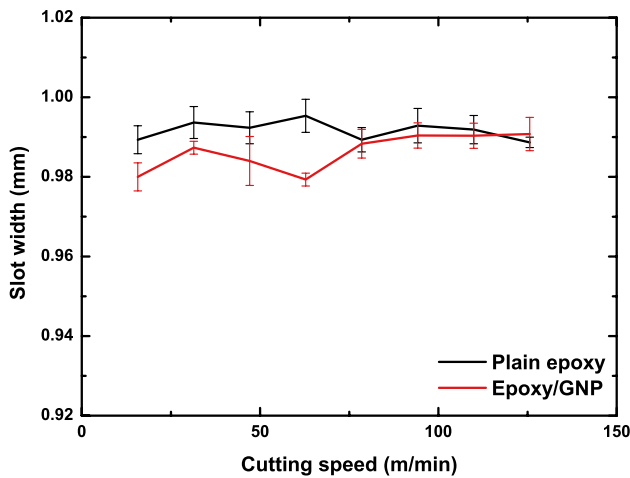


Fig. 9 Slot width value of plain epoxy and epoxy/GNP at cutting speeds from 15.7 to 125.6 m/min at 0.1 mm depth of cut

the thermosetting polymer are two competing mechanisms. The first ‘fall’ trend indicates that strain hardening is the dominant effect at the initial cutting speed, while the effects of thermal softening gradually come to dominate the cutting process as the speed increases. The ‘rise’ trend suggests that the epoxy chains reach the slip maximum and increase the cutting force, and strain hardening predominates again [28]. The addition of GNP nanoparticles will not affect this phenomenon.

Figure 11 also shows that the cutting force of epoxy/GNP is higher than that of plain epoxy. This may be two reasons for this. Firstly, the addition of GNP nanoparticles means that the matrix material will produce greater crack deformation during processing. Compared with plain epoxy, this will increase the total fracture surface area and thereby absorb more energy, leading to greater cutting force on the epoxy/GNP [50]. Secondly, the overall strength and modulus of the epoxy/GNP nanocomposite is greater, which also raises the cutting force [50]. However, there is little difference in cutting force between the two materials, possibly because the GNP nanoparticles act as a lubricant in the machining process and reduce the friction between the cutting edge and the workpiece [46]. This increase in lubrication performance could offset the effect of the greater overall strength and modulus of epoxy/GNP nanocomposite.

3.4 Shear stress

Due to the viscous behaviour of polymer materials, the mechanical properties of the polymer change significantly during the cutting process. Xiao and Zhang [16] demonstrated that the shear stress of the polymer increases with strain rate and cutting speed but decreases with temperature. Shear stress is a good indicator of the ultimate influence of strain rate and cutting speed. However, the impact

of nanoparticles on the shear stress of polymer has not been sufficiently investigated. The aim of this part of the study is to fill this gap.

According to the orthogonal model, shear stress may be expressed as in Eq. 2 [16]:

$$\tau_t = \frac{[(F_c \cos \varnothing) - (F_t \sin \varnothing)] \sin \varnothing}{A_c} \quad (2)$$

where τ_t is the average shear stress along the chip shear plane, A_c is the cross-sectional area of the uncut chip, and \varnothing is the shear angle.

Figure 12 shows a schematic of the orthogonal machining process, in which F_r is the resultant tool force, F_c is the cutting force, F_t is the thrust force, F_s is the shear force on the shear plane, \varnothing is the shear angle, γ is the normal working rake, a_c is the undeformed chip thickness, a_0 is the chip thickness, and l_s is the shear plane length. By using an optical microscope, the chip thickness was measured in this study.

Shear angle may be calculated as in Eq. 3 [16]:

$$\tan \varnothing = \frac{(a_c/a_0) \cos \gamma}{1 - (a_c/a_0) \sin \gamma} \quad (3)$$

where γ is the rake angle of the cutting tool, r_c is the cutting ratio, a_c is the undeformed chip thickness, and a_0 is the chip thickness.

Figure 13 presents SEM micrographs of the chip thickness, which was measured using ImageJ software, and each data point is obtained by randomly selecting five different positions on the same chip and averaging them. Figure 14 presents the chip thickness values from plain epoxy and epoxy/GNP in this study. Figure 15 shows the relationship between the shear stresses of plain epoxy and epoxy/GNP. Both present a trend of the shear stress observed to increase with cutting speed. Previous studies have concluded that the shear stress of plain polymer also increases with cutting speed [36], while metal machining research has shown that shear stress decreases slightly or is constant over a wide range of cutting speeds [35]. Therefore, the addition of GNP nanoparticles cannot significantly affect shear stress compared with that of plain epoxy. This means that the surface quality of both plain epoxy and epoxy/GNP will improve with increasing cutting speed. This conclusion is consistent with the experimental results shown in Fig. 8 and the findings of previous research [51, 52].

3.5 Tool wear

To provide more detailed information for industrial applications, tool wear needs to be measured. Previous studies have demonstrated a typical tool wear pattern occurring on the flank face of the milling tool [53]. Figure 16 shows the effect of GNP nanoparticles on the flank wear of uncoated tools.

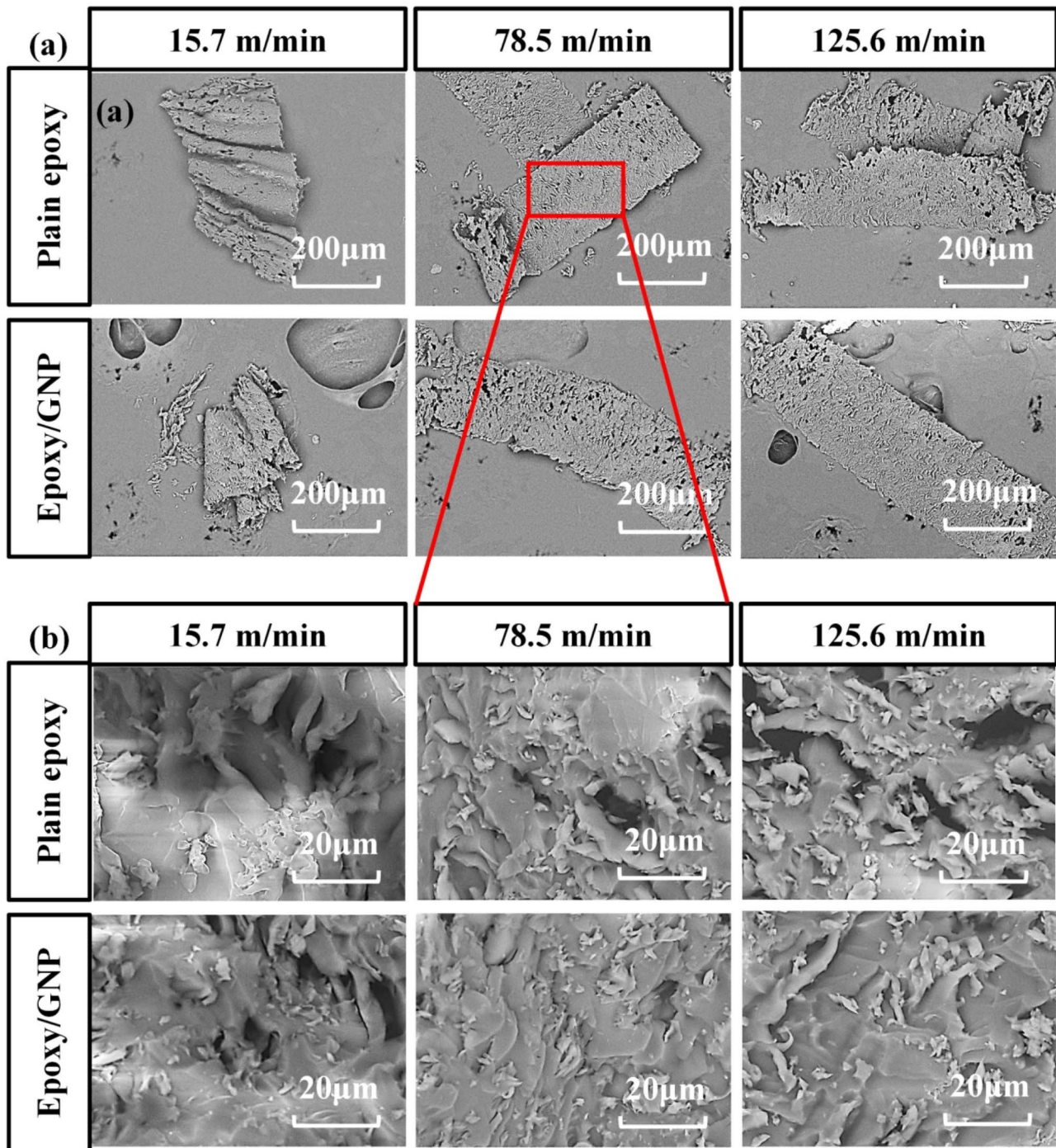


Fig. 10 SEM images of chips and chip surfaces at cutting speeds of 15.7, 78.5, and 125.6 m/min at 0.1 mm undeformed chip thickness: (a) chips; (b) chip surfaces

Tool wear is quantified based on the distance between the two red lines and measured using ImageJ. By adding GNP nanoparticles, the tool wear of uncoated tools is increased. The uncoated tool becomes gradually rounded, and there is no edge chipping at its edge. The flank wear for epoxy/GNP is 5 μm, and for plain epoxy 3 μm. In this study, two tools for removing workpiece material with a volume of

130 mm³ were used. Finally, the tool that has been used in this experiment was employed to cut a slot to study the impact of new and old tools on cutting accuracy at a cutting speed of 78.5 m/min. Figure 17 shows the effect of tool life on the surface roughness of epoxy/GNP and plain epoxy, and Fig. 18 shows the effect of tool life on slot width when machining epoxy/GNP and plain epoxy. However, compared

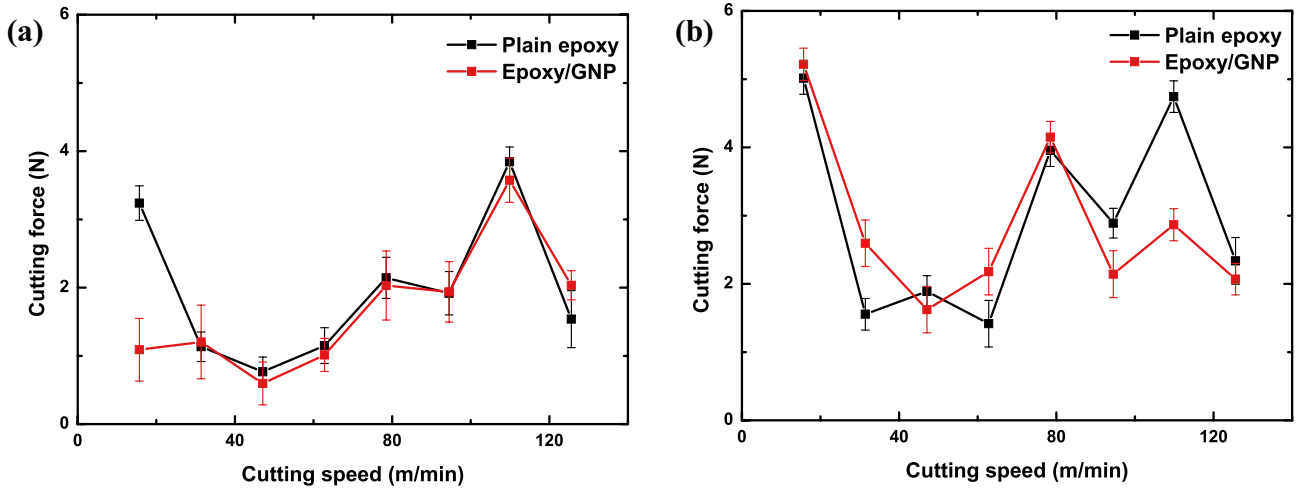


Fig. 11 Effect of GNP loading on cutting force at a depth of cut of (a) 0.1 mm and (b) 0.2 mm

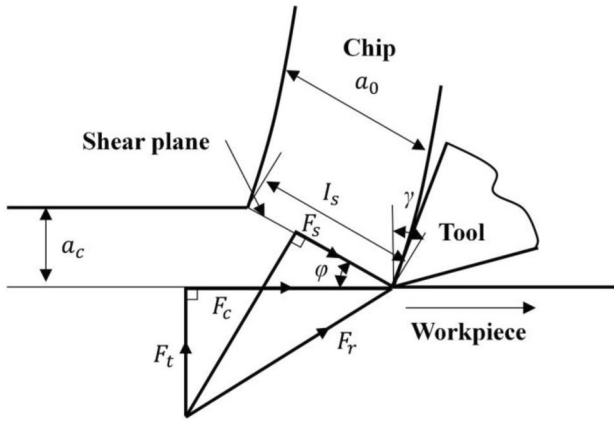


Fig. 12 Schematic of the orthogonal machining process

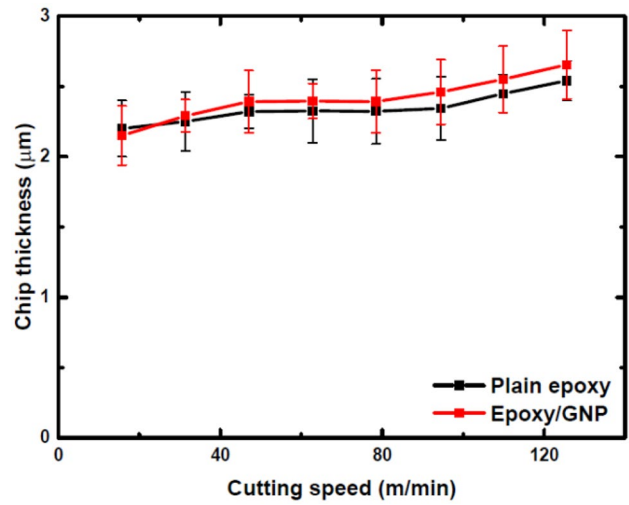
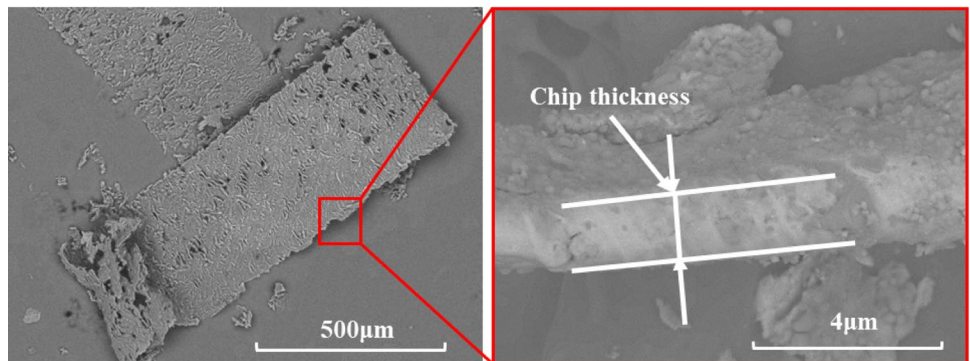


Fig. 14 Chip thickness values of plain epoxy and epoxy/GNP

Fig. 13 SEM micrographs of chip thickness



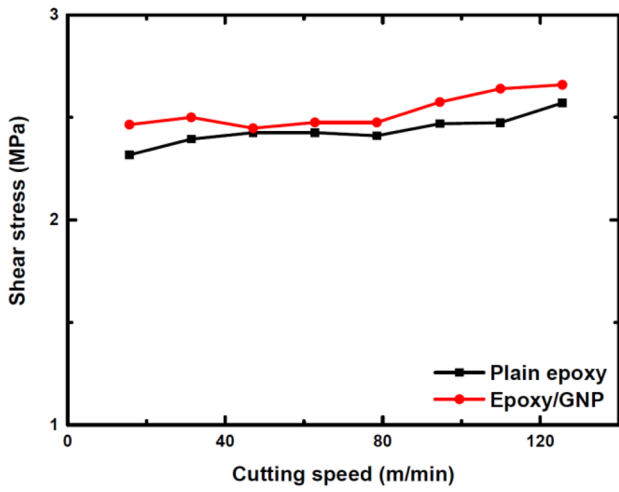


Fig. 15 Calculated shear stress of plain epoxy and epoxy/GNP at cutting speeds from 15.7 to 125.6 m/min at 0.1 mm depth of cut

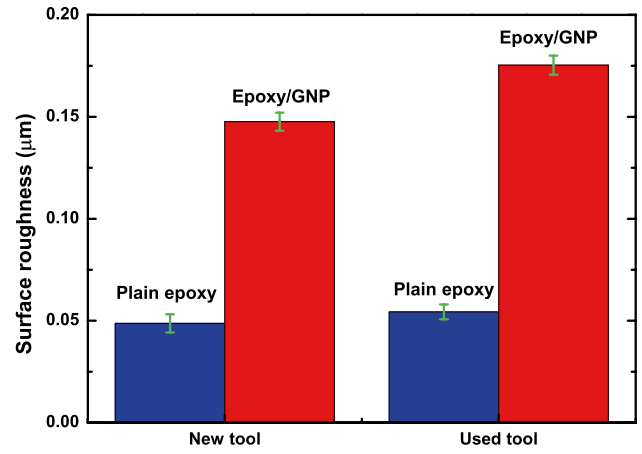
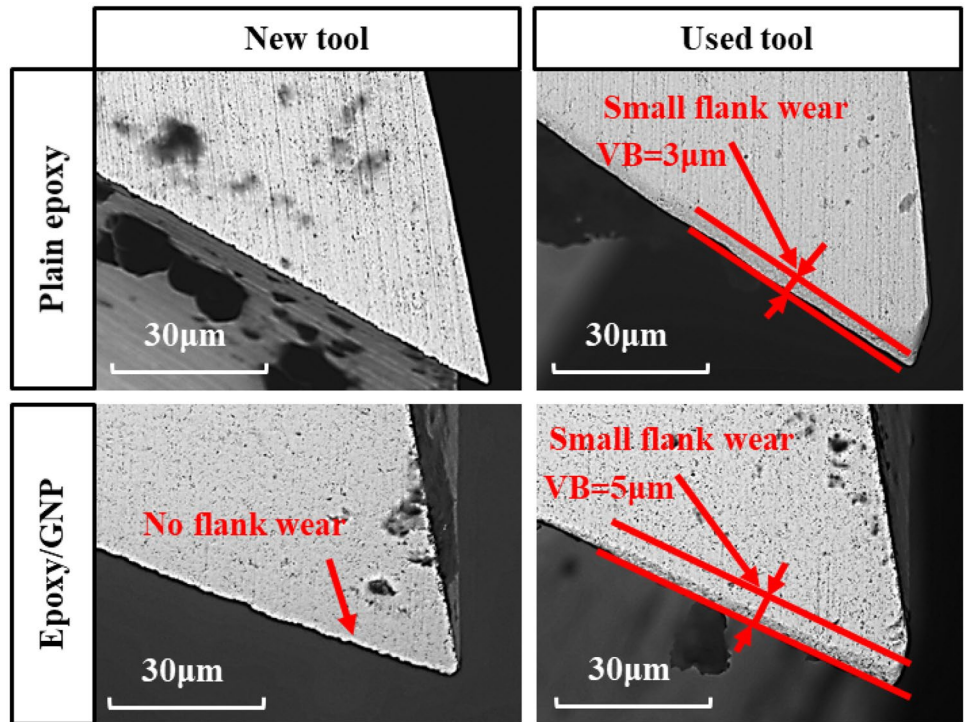


Fig. 17 Effect of tool life on the surface roughness of epoxy/GNP and plain epoxy

Fig. 16 SEM micrographs of tool flank wear



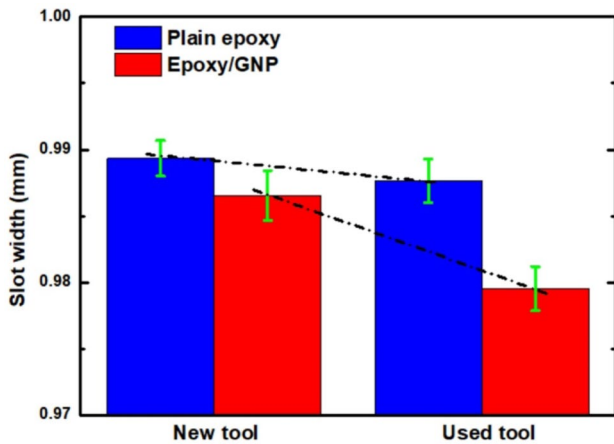


Fig. 18 Effect of tool life on slot width when machining epoxy/GNP and plain epoxy

with metal nanocomposites [53], the addition of GNP particles is thus considered insufficient to significantly affect the accuracy of the machined surface and the extra tool wear when micro-machining epoxy/GNP materials.

4 Conclusions

The micro-machinability of plain epoxy and epoxy/GNP nanocomposites has been investigated in micro-milling experiments with various cutting speeds. The results of machining for both materials are characterised in terms of surface roughness, surface morphology, cutting forces, shear stress, chip formation, slot width accuracy and tool wear. The following conclusions can be drawn:

- This fall-rise-fall trend of cutting force against cutting speed is like the behaviour of thermosetting polymer in macro-milling. The addition of GNP nanoparticles will not affect this phenomenon.
- The shear stress of epoxy/GNP and plain epoxy increases with the increase in the cutting speeds. A relatively large shear stress corresponds to a smoother machining surface of plain epoxy and epoxy/GNP.
- With the addition of GNP nanoparticles, the slot edge formation mode of the matrix material changes from burring mode to chipping mode. Both plain epoxy and epoxy/GNP show continuous chips with no significant difference between them.

Declarations

Ethics approval Not applicable.

Consent to participate All the authors give their permissions to participate and publish.

Consent for publication All the authors give their permissions to participate and publish.

Competing interests The authors declare no competing interests.

Open Access This article is licensed under a Creative Commons Attribution 4.0 International License, which permits use, sharing, adaptation, distribution and reproduction in any medium or format, as long as you give appropriate credit to the original author(s) and the source, provide a link to the Creative Commons licence, and indicate if changes were made. The images or other third party material in this article are included in the article's Creative Commons licence, unless indicated otherwise in a credit line to the material. If material is not included in the article's Creative Commons licence and your intended use is not permitted by statutory regulation or exceeds the permitted use, you will need to obtain permission directly from the copyright holder. To view a copy of this licence, visit <http://creativecommons.org/licenses/by/4.0/>.

References

1. Liu C, Yu Z, Neff D, Zhamu A, Jang BZ (2010) Graphene-based supercapacitor with an ultrahigh energy density. *Nano Lett* 10(12):4863–4868
2. Bonaccorso F, Colombo L, Yu G, Stoller M, Tozzini V, Ferrari AC, Ruoff RS, Pellegrini V (2015) Graphene, related two-dimensional crystals, and hybrid systems for energy conversion and storage. *Science* 347(6217):1246–1252
3. Hong N, Zhan J, Wang X, Stec AA, Hull TR, Ge H, Xing W, Song L, Hu Y (2014) Enhanced mechanical, thermal and flame retardant properties by combining graphene nanosheets and metal hydroxide nanorods for acrylonitrile–butadiene–styrene copolymer composite. *Compos Part A Appl Sci Manuf* 64:203–210
4. Rafiee MA, Lu W, Thomas AV, Zandiatashbar A, Rafiee J, Tour JM, Koratkar NA (2010) Graphene nanoribbon composites. *ACS Nano* 4(12):7415–7420
5. Domun N, Hadavinia H, Zhang T, Sainsbury T, Liaghat GH, Vahid S (2015) Improving the fracture toughness and the strength of epoxy using nanomaterials: a review of the current status. *Nanoscale* 7(23):10294–10329
6. Kumar MN, Mahmoodi M, TabkhPaz M, Park SS, Jin X (2017) Characterization and micro end milling of graphene nano platelet and carbon nanotube filled nanocomposites. *J Mater Process Technol* 249:96–107
7. Atif R, Wei J, Shyha I, Inam F (2016) Use of morphological features of carbonaceous materials for improved mechanical properties of epoxy nanocomposites. *RSC Adv* 6(2):1351–1359
8. Saharudin M, Shyha I, Inam F (2016) Viscoelastic and mechanical properties of multi-layered graphene polyester composites, In: *Proceedings of the 2nd International Conference on Advances in Mechanical Engineering, Istanbul, Turkey* 10–13
9. Atif R, Shyha I, Inam F (2016) Mechanical, thermal, and electrical properties of graphene-epoxy nanocomposites: a review. *Polymers* 8(8):281
10. López-Suárez M, Torres FM, Rurali R, Abadal G (2014) Fabrication of highly regular suspended graphene nanoribbons through a one-step electron beam lithography process. *Microelectron Eng* 118:81–85
11. Han MY, Özyilmaz B, Zhang Y, Kim P (2007) Energy band-gap engineering of graphene nanoribbons. *Phys Rev Lett* 98(20):206805

12. Novoselov KS, Jiang D, Schedin F, Booth TJ, Khotkevich VV, Morozov SV, Geim AK (2005) Two-dimensional atomic crystals. *Proc Natl Acad Sci* 102(30):10451–10453
13. Davanloo F, Miura Y, Macosko CW (2009) Graphene/polyurethane nanocomposites for improved gas barrier and electrical conductivity. *Nat Nanotechnol* 4(11):711–723
14. Fetecau C, Stan F, Munteanu A, Popa V (2008) Machining and surface integrity of polymeric materials. *Int J Mater Form* 1(1):515–518
15. Alauddin M, Choudhury IA, El Baradie MA, Hashmi MSJ (1995) Plastics and their machining: a review. *J Mater Process Tech* 54(1–4):40–46
16. Xiao KQ, Zhang LC (2002) The role of viscous deformation in the machining of polymers. *Int J Mech Sci* 44(11):2317–2336
17. Roy PK, Basu SK (1977) Evaluation of processing factors on turning of thermoplastics. *Polym Eng Sci* 17(10):751–757
18. Jiao F, Cheng K (2014) An experimental investigation on micro-milling of polymethyl methacrylate components with nanometric surface roughness. *Proc Inst Mech Eng Part B J Eng Manuf* 228(5):790–796
19. Samuel J, DeVor RE, Kapoor SG, Hsia KJ (2006) Experimental investigation of the machinability of polycarbonate reinforced with multiwalled carbon nanotubes. *J Manuf Sci Eng* 128(2):465
20. Kobayashi A (1967) *Machining of plastics*. McGraw-Hill, New York
21. Patel Y, Blackman BRK, Williams JG (2009) Measuring fracture toughness from machining tests. *Proc Inst Mech Eng Part C J Mech Eng Sci* 223(12):2861–2869
22. Jiang Q, Zhang LC, Pittolo M (2000) The dependence of surface finish of a spectacle polymer upon machining conditions. *Prog Mach Technol Aviat Ind Press Beijing* 7–12
23. Yan Y, Mao Y, Li B, Zhou P (2021) Machinability of the thermoplastic polymers: peek, pi, and pmma. *Polymers (Basel)* 13(1):69
24. Aramcharoen A, Sean SKC, Kui L (2012) An experimental study of micromilling of polymer materials for microfluidic applications. *Int J Abras Technol* 5(4):286–298
25. Crabtree P, Dhokia VG, Newman ST, Ansell MP (2009) Manufacturing methodology for personalised symptom-specific sports insoles. *Robot Comput Integr Manuf* 25(6):972–979
26. Davies MA, Burns TJ (2001) Thermomechanical oscillations in material flow during high-speed machining. *Philos Trans R Soc A Math Phys Eng Sci* 359(1781):821–846
27. Dikshit A, Samuel J, DeVor RE, Kapoor SG (2008) A microstructure-level material model for simulating the machining of carbon nanotube reinforced polymer composites. *J Manuf Sci Eng Trans ASME* 130(3)
28. Samuel J, Dikshit A, DeVor RE, Kapoor SG, Hsia KJ (2009) Effect of carbon nanotube (CNT) loading on the thermomechanical properties and the machinability of CNT-reinforced polymer composites. *J Manuf Sci Eng* 131(3):031008
29. Kobayashi A, Saito K (1962) On the cutting mechanism of high polymers. *J Polym Sci* 58(166):1377–1396
30. Xu J, Li C, Dang J, El Mansori M, Ren F (2018) A study on drilling high-strength CFRP laminates: frictional heat and cutting temperature. *Materials (Basel)* 11(12):2366
31. Le B, Kernin A, Khaliq J, Fu G, Huo D, Bilotti E, Zhang H, Shyha I (2021) Micro-end-milling of carbon nanotube reinforced epoxy nanocomposites manufactured using three roll mill technique. *J Manuf Process* 70:307–320
32. Shakoori N, Fu G, Le B, Khaliq J, Jiang L, Huo D, Shyha I (2021) An experimental investigation on tool wear behaviour of uncoated and coated micro-tools in micro-milling of graphene-reinforced polymer nanocomposites. *Int J Adv Manuf Technol* 113(7):2003–2015
33. Fu G, Huo D, Shyha I, Pancholi K, Alzahrani B (2020) Experimental investigation on micromachining of epoxy/graphene nano platelet nanocomposites. *Int J Adv Manuf Technol* 107(7):3169–3183
34. Shyha I, Fu GY, Huo DH, Le B, Inam F, Saharudin MS, Wei JC (2018) Micro-machining of nano-polymer composites reinforced with graphene and nano-clay fillers. *Key Eng Mater* 786:197–205
35. Lai X, Li H, Li C, Lin Z, Ni J (2008) Modelling and analysis of micro scale milling considering size effect, micro cutter edge radius and minimum chip thickness. *Int J Mach Tools Manuf* 48(1):1–14
36. Wei J (2017) Graphene in epoxy system: dispersion, preparation and reinforcement effect. Ph.D. thesis (unpubl.), Northumbria University, Newcastle upon Tyne, UK
37. Teng X, Huo D, Wong E, Meenashisundaram G, Gupta M (2016) Micro-machinability of nanoparticle-reinforced Mg-based MMCs: an experimental investigation. *Int J Adv Manuf Technol* 87(5–8):2165–2178
38. Kumar MN, Mahmoodi M, TabkhPaz M, Park SS, Jin X (2017) Characterization and micro end milling of graphene nano platelet and carbon nanotube filled nanocomposites. *J Mater Process Technol* 249:96–107
39. Gao C, Jia J (2017) Factor analysis of key parameters on cutting force in micromachining of graphene-reinforced magnesium matrix nanocomposites based on FE simulation. *Int J Adv Manuf Technol* 92:9–12
40. Atif R, Shyha I, Inam F (2017) Modeling and experimentation of multi-layered nanostructured graphene-epoxy nanocomposites for enhanced thermal and mechanical properties. *J Compos Mater* 51(2):209–220
41. Rafiee MA, Rafiee J, Yu ZZ, Koratkar N (2009) Buckling resistant graphene nanocomposites. *Appl Phys Lett* 95(22):223103
42. Srivatsan TS (2009) A review of: Fractography: observing, measuring, and interpreting fracture surface topography, by D. Hull. *Mater Manuf Process* 1229
43. Geoffrey B (1975) *Fundamentals of metal machining and machine tools*. McGraw-Hill, New York
44. Schaller T, Bohn L, Mayer J, Schubert K (1999) Microstructure grooves with a width of less than 50 μm cut with ground hard metal micro end mills. *Precis Eng* 23(4):229–235
45. Kobayashi A (1984) Ultra-precision machining of plastics. *Production Aspects of Single Point Machined Optics* 508:31–38
46. Carr JW, Feger C (1993) Ultraprecision machining of polymers. *Precis Eng* 15(4):221–237
47. Altıntaş Y, Budak E (1995) Analytical prediction of stability lobes in milling. *CIRP Ann - Manuf Technol* 44(1):357–362
48. Arora I, Samuel J, Koratkar N (2013) Experimental investigation of the machinability of epoxy reinforced with graphene platelets. *J Manuf Sci Eng* 135(4):041007
49. Saito K (1981) Fracture phenomena of high polymers in cutting. *J Macromol Sci Part B* 19(3):459–485
50. Rafiee MA, Rafiee J, Srivastava I, Wang Z, Song H, Yu ZZ, Koratkar N (2010) Fracture and fatigue in graphene nanocomposites. *Small* 6(2):179–183
51. Chao BT, Bisacre GH (1951) The effect of speed and feed on the mechanics of metal cutting. *Proc Inst Mech Eng* 165(1):1–13
52. Wallace PW (1962) An investigation on the friction between chip and tool in metal cutting Fellowship thesis. *Dep Mech Eng Univ Salford Engl*
53. Teng X, Huo D, Shyha I, Chen W, Wong E (2018) An experimental study on tool wear behaviour in micro milling of nano Mg/Ti metal matrix composites. *Int J Adv Manuf Technol* 96(5–8):2127–2140